Dynamic study of conduction carriers in $YBa_2Cu_3O_{7-\delta}$ thin films using a pulsed-laser-induced transient-thermoelectric-effect method

M. Sasaki, G. X. Tai, S. Tamura, and M. Inoue
Department of Materials Science, Faculty of Science, Hiroshima University, Higashi-Hiroshima 724, Japan
(Received 26 March 1991; revised manuscript received 30 December 1991)

The pulsed-laser-induced transient thermoelectric effect (TTE) has been measured for *c*-axis-oriented $YBa_2Cu_3O_{7-\delta}$ thin films over a wide time range (50 ns to 2 ms) and temperature range (10–300 K). The analysis of the decay curves of TTE voltages has revealed that the $YBa_2Cu_3O_{7-\delta}$ system has multiple conduction carriers, the semiconducting holes in the one-dimensional (1D) CuO chains and two types of holes (light-mass and heavy-mass holes) arising from the metallic 2D CuO_2-derived band. From the observed relaxation times for thermal diffusions of light and heavy holes, we have estimated their mobilities, which show a "critical slowing-down"-like anomaly near the superconducting transition temperature T_c. The temperature dependence of the hole mobilities can be reasonably explained by considering a critical divergent nature of the diffusion coefficients for conduction holes and a "quasiparticle lifetime" τ^* in the superconducting state. In the superconducting state we have observed the stepwise-, shunt-, and plateau-type TTE signals above and/or below a characteristic temperature T_c^* ($=35$ K). The presence of T_c^* is indicative of an additional superconducting transition from phase I to II of the quasiparticle system.

I. INTRODUCTION

Since the work of high-T_c layered copper oxide superconductors by Bednorz and Müller,[1] various experimental techniques have been employed to study electronic properties of numerous high-T_c materials, using traditional methods of static transport, magnetic, thermal measurements, as well as modern techniques such as neutron diffraction and photoemission spectroscopy. However, the fundamental understanding of the superconducting mechanism is still uncertain.

Recently we have developed a technique called transient-thermoelectric-effect (TTE) method using pulsed-laser light.[2] This technique, based on a very simple working principle, is a powerful method, we believe, to obtain dynamic information on conduction carriers and phonons in various solids.[2–6] In principle, when pulsed-laser light irradiates one end of a sample, one measures an induced TTE voltage across both ends of the sample, and can analyze its decay profiles to get valuable information about the carrier generation-recombination process and the thermal diffusions of photogenerated carriers (and phonons) drifting along the concentration and temperature gradient in the sample.

Our preliminary experiment has shown that this method is also applicable to high-T_c superconductors such as $YBa_2Cu_3O_{7-\delta}$ thin films;[5] we have provided direct evidence for "two kinds of holes" existing near the Fermi energy E_F, in agreement with theoretical predictions by Massidda, Yu, and Freeman.[7] Similar measurements of laser-induced voltages for unbiased and biased $YBa_2Cu_3O_{7-\delta}$ thin films have been made by Chang *et al.*,[8,9] in which special attention has been paid to the decay profiles in the short-time interval 0–500 ns; they attribute it to a local structure of the film itself, but not to a bolometric effect. In the present work, we shall show more detailed data obtained with a controlled laser intensity and discuss quantitatively on the dynamic properties of multiple conduction carriers in $YBa_2Cu_3O_{7-\delta}$ thin films.

II. EXPERIMENTAL

The samples of high-quality *c*-axis-oriented $YBa_2Cu_3O_{7-\delta}$ (YBCO) thin films (thickness $d \sim 200$ nm; critical temperature $T_c = 82$ K) grown *in situ* on a yttrium-stabilized zirconia (100) substrate (YBCO/ZrO_2) using an off-axis single-target magnetron sputtering technique, were provided by T. H. Geballe and co-workers.[10]

The experimental setup and measuring principle are described elsewhere.[2] A pulsed laser produced by a Nd-doped glass laser source (laser power: ~ 1 J) with the wavelength of 1.06 μm ($=1.17$ eV) and pulsewidth of 25 ns was irradiated normal to one end of a thin film (typically 2 mm long and 0.5 mm wide) through a slit of about 0.8 mm, as shown in Fig. 1.

Electrical leads to both ends of a sample film were soldered by an indium metal. The laser-induced TTE volt-

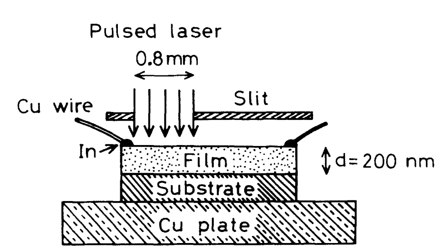

FIG. 1. Schematic arrangement for a pulsed laser irradiation upon a YBCO film deposited on a substrate.

age across a sample was detected over the wide time range 50 ns–2 ms by a digital storage oscilloscope through a home-made preamplifier, whose output signal was fed to a computer for record and numerical analysis. We have confirmed that the TTE voltage does not depend on a sample size (length and width).

The laser intensity I at the sample position (illuminated area: about 0.8×0.5 mm^2) was controlled by an optical lens system and checked by a commercial Fast-Response Joulemeter (Genetec, Inc., model ED-200). In the present experiments we have employed relatively weak laser intensity $I = 0.3$–12 mJ/cm^2 to avoid thermal heating or bolometric effect of the laser light on the YBCO films. In fact, a rough evaluation of the photogenerated temperature rise $\Delta(T)$ under these laser illuminations using standard heat transfer calculations shows that the values of $\Delta(T)$ are at most within a few kelvins, and the heat is dissipated within 50–100 ns through the zirconia substrate; here we have used the known values of heat capacity[11] and thermal conductivities of YBCO (Ref. 12) and zirconia.[13] Thus we may conclude that under the present experimental conditions, a thermal equilibrium is readily established across the YBCO films within 50–100 ns, beyond which the heating or bolometric effect can be neglected.

III. RESULTS

The decay curves of photoinduced TTE signals are strongly dependent on both temperature T and laser intensity I, as schematically shown in Fig. 2 for the as-grown $YBCO/ZrO_2$ ($T_c = 82$ K) sample; similar behaviors are also observed for their vacuum-annealed samples (annealing temperature $T_A = 100$–$300\,^\circ$C) and for $YBa_2Cu_3O_{7-\delta}$ films grown on a $SrTiO_3$ substrate.[5] The characteristic features of these profiles are described as follows.

A. Low laser intensity $I \leq 1$ mJ/cm^2

(i) At 300 K, the photoinduced TTE voltage V rises drastically to a few mV within a short period ($\sim$ 50 ns)

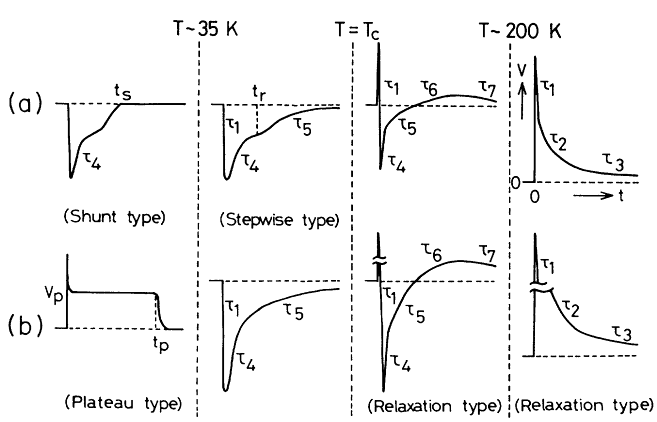

FIG. 2. Characteristic decay profiles of the TTE voltages V for the as-grown $YBCO/ZrO_2$ film at (a) lower ($I \leq 1$ mJ/cm^2) and (b) higher ($I \geq 1$ mJ/cm^2) laser intensities. These profiles show anomalies around 200 and 35 K.

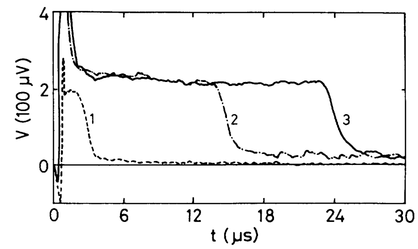

FIG. 3. Plateau-type TTE voltages at 10 K for the as-grown $YBCO/ZrO_2$ at different laser intensities I. (1) $I = 0.76$ mJ/cm^2, (2) $I = 3.6$ mJ/cm^2, and (3) $I = 6.3$ mJ/cm^2.

and decays exponentially with some characteristic relaxation times τ_1–τ_3. (ii) Around 200 K, the TTE voltage changes its sign (from positive to negative), and below about 200 K, τ_2 and τ_3 become gradually undetectable, while the relaxation process with τ_1 continues to have a large relaxation amplitude, but (iii) below 200 K through T_c, the decay curve is described by additional relaxation times τ_4–τ_7, where these processes are observed over a wide time interval 0.5 μs–2 ms. (iv) Below T_c, the decay curve exhibits a "stepwise-type" form with two relaxation times τ_4 and τ_5 and with a characteristic transition time t_r, the observable range of which is approximately $35 < T < 65$ K. (v) At lower temperatures $T < 35$ K, the TTE voltage is completely shunted to zero within a "shunt time" t_s that depends slightly on temperature (see Fig. 8).

B. High laser intensity $I > 1$ mJ/cm^2

Notable features of the TTE decay curves at high laser intensity are (vi) the blur or disappearance of the stepwise form observed in the temperature range between 35 and 65 K, and (vii) the appearance of a "plateau-type" TTE curve detected solely at lower temperatures $T < 35$ K, as illustrated in some detail in Fig. 3, the data being taken at 10 K for three fixed laser intensities $I = 0.76$, 3.6, and 6.3 mJ/cm^2. With increasing intensity I, the plateau lasts for a longer time (denoted by "plateau time", t_p), but with nearly constant TTE voltage (denoted by "plateau voltage", V_p). In Fig. 4, these values obtained at 10, 20,

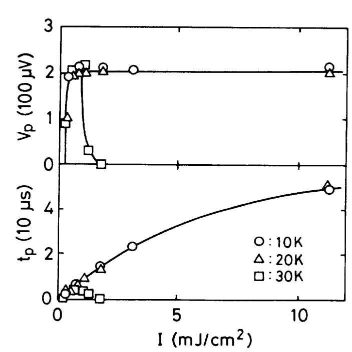

FIG. 4. Laser intensity dependence of the plateau voltage V_p and plateau time t_p for the as-grown $YBCO/ZrO_2$ at three fixed temperatures 10, 20, and 30 K.

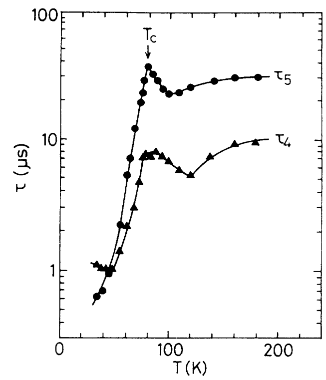

FIG. 5. Temperature dependence of the relaxation times τ_4 and τ_5 for the as-grown YBCO/ZrO_2.

and 30 K are plotted against the laser intensity I. We see that at 10 and 20 K, with increasing I the plateau voltage V_p is raised sharply and then kept at a constant value $V_p \sim 200$ μV, while the plateau time t_p increases monotonically with the laser intensity I; at 30 K both V_p and t_p vanish for higher laser intensities $I > 2$ mJ/cm^2.

Now the temperature dependence of the observed relaxation times has been already reported in previous work.[5] Of particular interest to note is that with decreasing temperature the relaxation times τ_4 and τ_5 shown in Fig. 5 increase exceedingly below 100 K and decrease drastically below T_c, indicating a "critical slowing-down"-like behavior near T_c. Furthermore, we have found that the stepwise curve described in (iv) consists of two exponentially decreasing functions with the relaxation times τ_4 and τ_5, which are connected with an appropriate transition function.[5] From the analysis of these functions, we have evaluated the superconducting gap energy $\Delta(T)$, whose temperature dependence follows approximately the conventional mean-field BCS curve. Finally, we note that at the normal state ($T > T_c$), the positive and nonvanishing TTE voltage of a few μV is observed in the long-time ranges more than 2 ms, which is due to a static thermopower produced by the laser-induced temperature difference ΔT across both ends of the sample; the value of ΔT estimated using a static thermopower[14] is less than 1 K.

IV. DISCUSSION

A. Relaxation process

Our pulsed-laser-induced TTE experiments have revealed the existence of various decay or relaxation processes with the characteristic relaxation times τ_i ($i = 1$–7) in the YBCO/ZrO_2 thin films (Fig. 2). From the observed differences in the magnitude of τ_i and of the relaxation amplitude a_i, their temperature dependence, and the annealing effect, the possible mechanism of light-generated carrier relaxations and of high-T_c superconductivity can be deduced, as given qualitatively below.[5]

(i) The decay processes $i = 1$–3 are due to a normal recombination of photogenerated electrons and holes via some ionized impurity centers, which are attributed to at least two types of Cu^{2+} ions located in the one-dimensional (1D) CuO chains, as found in various semiconductors.[2–4] According to a conventional recombination mechanism,[15] the evaluated recombination time τ_r is of the order of 100 ns, which is comparable order of magnitude to the observed values of τ_1–τ_3.

(ii) The decay processes $i = 4$–7 are the carrier diffusion of the photogenerated excess electrons and holes.[5] In particular, the relaxation times τ_4 and τ_5 show a "critical slowing-down"-like behavior near T_c (Fig. 5). As will be discussed in Sec. IV B, τ_4 and τ_5 can be assigned to light-mass and heavy-mass holes existing near the Fermi energy E_F, respectively, in good agreement with recent band calculations for YBCO by Massidda, Yu, and Freeman.[7] A recent report on the quantum oscillations with two components in YBCO also suggests the presence of two kinds of holes near E_F.[16]

B. Evaluation of light- and heavy-hole mobilities

From the observed relaxation times τ_4 and τ_5 for thermal diffusions of photogenerated carriers (holes), we can evaluate the corresponding carrier mobilities μ_i ($i = 4,5$). According to our previous analysis,[2] τ_i and μ_i are expressed as

$$\tau_i = L_i^2/(2D_i), \quad \mu_i = eL_i^2/(2k_B T \tau_i) , \tag{1}$$

where L_i is a diffusion length for the ith relaxation process, D_i ($= k_B T \mu_i / e$) the diffusion coefficient, and k_B the Boltzmann constant. We assume that the diffusion length of heavy holes is the same as that of light holes, and then we set $L_i = L$. Unfortunately, there are no available data for the diffusion length L for YBCO. Here we have used the empirical expression found for $M_x TiS_2$ (M = transition metal,[3] $L = 1.3 \times 10^{-9} B^{-1} T^{1/3}$, where B is a temperature gradient of an electrical resistivity ρ; we note that the carrier concentrations of $M_x TiS_2$ and YBCO (Ref. 17) are nearly equal ($\sim 10^{20}$–10^{22} cm^{-3}).

With the values of B obtained from the observed ρ-T curve (Fig. 7) and τ_i (Fig. 5), we have evaluated the light-mass ($i = 4$) and heavy-mass ($i = 5$) mobilities μ_l (solid circles) and μ_h (open circles), respectively, as illustrated in Fig. 6. In the normal state ($T > T_c$), μ_l and μ_h obey the power law of $T^{-1.0}$ and $T^{-1.6}$, respectively; the latter power law is nearly the same as T^{-2} obtained from the static Hall-effect measurements.[17] Furthermore, it is surprising that our light-hole mobility μ_l is nearly equal to that predicted by Stomer *et al.* from the resistivity, Hall-effect, and magnetoresistance data.[17] We see that with decreasing temperature both μ_l and μ_h show a critical slowing-down-like behavior near T_c (see later discussion Sec. IV C).

Using such two types of conduction holes with mobilities μ_l and μ_h, we have attempted to simulate the temperature dependence of the resistivity ρ in the normal state, according to

$$\rho = [e(p_l \mu_l + p_h \mu_h)]^{-1} , \tag{2}$$

where p_l and p_h are the carrier concentration for light

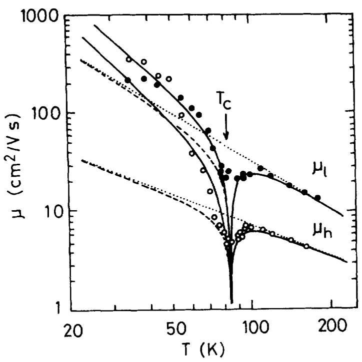

FIG. 6. Temperature dependence of the light- and heavy-hole mobilities μ_l (solid circles) and μ_h (open circles) estimated using Eq. (1) for the as-grown $YBCO/ZrO_2$. The dotted lines are the ones calculated by Eq. (1) in the normal state, the broken lines by Eq. (1) under consideration of a critical slowing-down effect of Eq. (3) around T_c, and the solid lines by Eq. (5), which takes account of a quasiparticle lifetime (see text).

and heavy holes, respectively. The simulated result for the as-grown $YBCO/ZrO_2$ film is shown in Fig. 7 by solid lines, which are in good agreement with the experimental data except for the region of superconducting fluctuation (~ 100 K). Here the carrier concentrations p_l and p_h are assumed to be independent of temperature, the best-fit values being $p_l = 2.2 \times 10^{20}$ cm^{-3} and $p_h = 3.8 \times 10^{20}$ cm^{-3}. The above results support that the two-carrier model is reasonable for YBCO thin films.

C. Critical slowing-down and quasiparticle lifetime

As described in Sec. IV B, the relaxation times τ_4 and τ_5 show the critical slowing-down-like behavior near T_c, which is the first observation of the critical phenomena in the electronic properties of the YBCO system. Here we shall ascribe the critical divergence to the diffusion coefficients D_i in Eq. (1) as a response coefficient due to a long-range-order correlation between normal carriers interacting with phonons, as

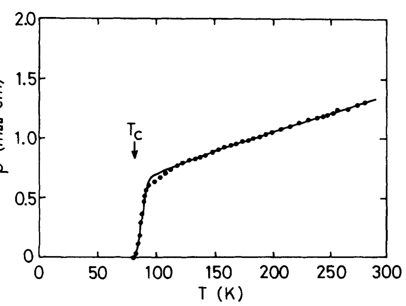

FIG. 7. Temperature dependence of the observed resistivity ρ for the as-grown $YBCO/ZrO_2$; the solid line is the one calculated using Eq. (2) with $p_l = 2.2 \times 10^{20}$ cm^{-3} and $p_h = 3.8 \times 10^{20}$ cm^{-3}.

$$D_i = D_i^N (1 + \epsilon |\Delta T_r|^{\delta}) , \quad (3)$$

where D_i^N is the diffusion coefficient in the normal state, ϵ a parameter, ΔT_r a reduced temperature $[=(T - T_c)/T_c]$, and δ a critical exponent. The calculated hole mobilities μ_i for the as-grown $YBCO/ZrO_2$ film are shown by the dashed lines in Fig. 6, with the best-fit values of $\epsilon = 0.08$ and $\delta = +1$ for both μ_h and μ_l. The dotted straight lines are the extrapolated ones from the normal states. The calculated curves are in good agreement with the experimental results, except at low temperatures.

In the superconducting state, upon irradiation of a pulsed laser (photon energy $= 1.17$ eV), electrons are excited spontaneously from the lower-lying band through a superconducting gap energy $\Delta(T)$ to a higher energy level, in the sense of a conventional BCS model, and these excited electrons will be cooled down by multiple phonon scatterings within an extremely short time (10^{-12}–10^{-15} s), which will subsequently recombine with some of "hole Cooper pairs" in the upper band. This leads to a breaking of hole Cooper pairs and thus the formation of unpaired holes, producing "quasiparticles." As pointed out by Tinkham,[18] the "quasiparticles" in a nonequilibrium state may form in a "quasiparticle potential," which is responsible for the observed TTE voltages in the superconducting state (Fig. 2). The disagreement between the experimental results and the theoretical curves far below T_c in Fig. 6 may result from the contribution of a lifetime τ^* of such quasiparticles to the hole mobilities, as discussed below.

The quasiparticle lifetime τ^* has been predicted theoretically by Chen, Wang, and Teng,[19] as given by

$$\tau^* = [4 k_B T / \pi \Delta(T)] \tau_{E,\mathrm{eff}} , \quad (4)$$

where $\tau_{E,\mathrm{eff}}$ is an effective electron-phonon correlation time. Thus, taking into account this contribution, we introduce an "effective" mobility μ_i^* below T_c, defined by

$$\mu_i^* = \mu_i^N + eL^2 / 2 k_B T \tau^* , \quad (5)$$

where μ_i^N is the mobility of normal carriers. According to Chen, Wang, and Teng,[19] the inelastic electron-phonon correlation times τ_E for normal metals lie in the time range $\tau_E = 10^{-10}$–10^{-8} s. However, multiple interactions of quasiparticles with phonon or Cooper pairs may occur during the carrier diffusion in the TTE process, and thus the effective electron-phonon correlation time $\tau_{E,\mathrm{eff}}$ may increase appreciably ($\tau_{E,\mathrm{eff}} \sim 1$ μs $\gg \tau_E$). The estimated values of the effective hole mobilities μ_i^* are shown by the solid curves in Fig. 6, where $\tau_{E,\mathrm{eff}} = 2.3$ μs is used and $\Delta(T)$ is evaluated according to the usual BCS theory.[5] Such correction can be satisfactorily fitted to our experimental results.

D. Shunt- and plateau-type decay curves

Figure 8 shows the temperature dependence of the quasiparticle lifetime τ^* of Eq. (4) used in the present analysis, together with the observed values of "shunt time" t_s (Fig. 2), plotted in semilogarithmic scales. As

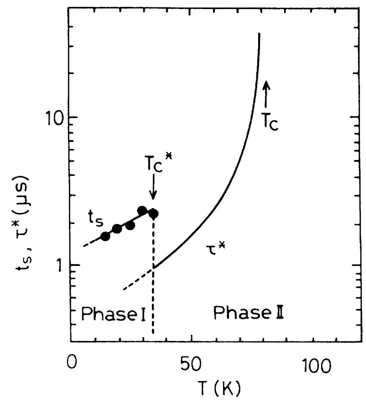

FIG. 8. Temperature dependence of the quasiparticle lifetime τ^* of Eq. (4) used in the present analysis and the observed shunt time t_s (Fig. 2) for the as-grown $YBCO/ZrO_2$ thin film. It is expected that the quasiparticle system undergoes a superconducting phase transition from phase I to II at the characteristic temperature of $T_c^* = 35$ K.

mentioned in Sec. III, the TTE voltage at a weak laser intensity $I \leq 1$ mJ/cm^2 is shunted completely after the characteristic "shunt time" t_s, while at high laser intensity $I \geq 1$ mJ/cm^2 such a shunt-type behavior disappears and instead a plateau-type decay curve appears. These behaviors are observed solely below 35 K (here we refer to a characteristic transition temperature T_c^*).

At present we cannot account for the physical origin of these shunt- and plateau-type behaviors observed below T_c^*. However, we should note that some anomalies in NQR (Ref. 20) and H_{c1} (Ref. 21) for YBCO are observed around T_c^*. In view of these experimental facts, we may expect that the quasiparticle system undergoes a superconducting phase transition from phase I to II at T_c^*. Further studies are required to confirm such a phase transition.

V. CONCLUSIONS

Pulsed-laser-induced "transient-thermoelectric-effect (TTE)" technique has been successfully applied to c-axis-oriented YBCO thin films. The analysis of the TTE decay curves has revealed that the YBCO system has multiple conduction carriers, the semiconducting holes in the 1D CuO chains and the metallic light and heavy holes near the Fermi energy of the 2D CuO_2 derived band. From the observed relaxation times for thermal diffusions of the photogenerated light and heavy holes, we have estimated their mobilities, which show a "critical slowing-down"-like behavior near the superconducting transition temperature T_c. The temperature dependence of the hole mobilities can be reasonably explained by taking account of a divergent nature of the diffusion coefficients for thermal diffusions of the mobile carriers and "quasiparticle lifetime" τ^* in the superconducting state. The thermal diffusion is thus considered to be due to the photogenerated "quasiparticles" drifting along a "quasiparticle potential."

Furthermore, in the superconducting state, we have observed the stepwise-, shunt-, and plateau-type TTE signals above and/or below 35 K ($=T_c^*$). The presence of the characteristic temperature T_c^* found in the present work may suggest that the quasiparticle system undergoes a second superconducting transition from phase I to II. In addition, the anomalies in the TTE voltages observed near 200 K may be related to the order-disorder transition of oxygen vacancies in the 1D CuO chains, as found by other workers.[22] More detailed measurements are required for further understanding of the "quasiparticle" picture and thus superconducting mechanism in high-T_c materials.

ACKNOWLEDGMENTS

We would like to express our sincere thanks to Professor T. H. Geballe, Stanford University, for providing us with the high-quality YBCO thin films used in the present work and valuable suggestions. We also thank Dr. K. Maeda (Sumitomo Kinzoku Kozan Co. Ltd.) for the use of a fast-response joulemeter, Dr. H. Negishi and Dr. M. Koyano for their useful discussions, and S. Yamamoto for his helpful assistance in taking the experimental data. Part of this work was financially supported by National Research Institute for Metals, Ogasawara Science Foundation, and Matsushita Elect. Ind. Co.

[1]J. G. Bednorz and K. A. Müller, Z. Phys. B **64**, 189 (1986).
[2]M. Sasaki, H. Negishi, and M. Inoue, J. Appl. Phys. **59**, 796 (1986).
[3]M. Sasaki, M. Koyano, and M. Inoue, J. Appl. Phys. **61**, 2267 (1987).
[4]M. Sasaki, S. Horisaka, and M. Inoue, Jpn. J. Appl. Phys. **26**, 1704 (1987).
[5]M. Sasaki, M. Koyano, H. Negishi, and M. Inoue, in *Science and Technology of Thin Film Superconductors 2,* edited by R. D. McConnell and R. Noufi (Plenum, New York, 1990), p. 517.
[6]M. Sasaki, G. X. Tai, and M. Inoue, Phys. Status Solidi B **162**, 553 (1990).
[7]S. Massidda, J. Yu, and A. J. Freeman, Phys. Lett. **122**, 198 (1987).
[8]C. L. Chang, A. Kleinhammes, W. G. Moulton, and L. R. Testardi, Phys. Rev. B **41**, 11 564 (1990).
[9]A. Kleinhammes, C. L. Chang, W. G. Moulton, and L. R. Testardi, Phys. Rev. B **44**, 2313 (1991).
[10]C. B. Eom, J. Z. Sun, K. Yamamoto, A. F. Marshall, K. E. Luther, T. H. Geballe, and S. S. Ladermann, Appl. Phys. Lett. **55**, 595 (1989).
[11]T. Lägreid, K. Fossheim, E. Sandvold, and S. Julsrud, Nature **330**, 637 (1987).
[12]S. J. Hagen, Z. Z. Wang, and N. P. Ong, Phys. Rev. B **40**, 9389 (1989).
[13]D. A. Ackerman, D. Moy, R. C. Potter, and A. C. Anderson, Phys. Rev. B **23**, 3886 (1981).
[14]S. Yan, P. Lu, and Q. Li, Solid State Commun. **65**, 355 (1988).
[15]G. Bemski, Phys. Rev. **111**, 1515 (1958).

[16]F. M. Mueller, C. M. Fowler, B. L. Freeman, W. L. Hults, L. C. King, and J. L. Smith (unpublished).

[17]H. L. Stomer, A. F. J. Levi, K. W. Baldwin, M. Anzlower, and G. S. Boebinger, Phys. Rev. B **38**, 2472 (1988).

[18]M. Tinkham, Phys. Rev. B **6**, 1747 (1972).

[19]L. Chen, G. Wang, and M. Teng, Phys. Status Solidi B **157**, 411 (1990).

[20]M. Tei, H. Takai, K. Mizoguchi, and K. Kume, Solid State Commun. **74**, 1117 (1990).

[21]J. P. Ströbel, M. Simmerl, H. Adrian, A. Thomä, G. Adrian, B. Hensel, and G. Saemann-Ischenko, Phys. C **153-155**, 1537 (1988).

[22]J. Toulouse, X. M. Wang, and D. J. L. Hong, Phys. Rev. B **38**, 7077 (1988).